

# Egg albumin as a nanoreactor for growing single-crystalline Fe<sub>3</sub>O<sub>4</sub> nanotubes with high yields†

Baoyou Geng,\* Fangming Zhan, Han Jiang, Yijun Guo and Zhoujing Xing

Received (in Cambridge, UK) 29th July 2008, Accepted 3rd September 2008

First published as an Advance Article on the web 1st October 2008

DOI: 10.1039/b813071j

**Single-crystalline Fe<sub>3</sub>O<sub>4</sub> nanotubes have been synthesized successfully by using egg albumin as a nanoreactor; these three-dimensional material nanotubes are formed through a rolling mechanism under mild biological conditions.**

In recent years considerable attention has been focused on one-dimensional (1D) nanostructured materials owing to their unique physical properties and potential applications. In particular, tubular-structured materials have shown unique chemical and physical properties because of their having outer as well as inner surfaces and a nanometre thick “wall”. Much effort has been devoted to the controllable synthesis of inorganic nanotubes since the discovery of carbon nanotubes in 1991.<sup>1</sup> The synthesis of a number of tubular materials from two-dimensional layered precursors at elevated temperatures, based on a “rolling-up” mechanism, has been reported,<sup>2</sup> such as those made from BN, V<sub>2</sub>O<sub>5</sub>, WS<sub>2</sub>, and NiCl<sub>2</sub>. Nanotubes made from other materials,<sup>3</sup> such as Si, ZnS, Eu<sub>2</sub>O<sub>3</sub>, and GaN, which do not possess 2D layered structures, have also been prepared by employing various hard templates. However, except for a few examples,<sup>3,4</sup> the template-assisted method has been proved to be unsuitable for the formation of single-crystalline nanotubes. A mild solution strategy has been used to obtain single-crystalline hexagonal prismatic Te nanotubes,<sup>5</sup> but it is difficult to extend this method to the formation of other three-dimensional materials. It is therefore still a challenge to extend the fabrication of single-crystalline tubular nanostructures from lamellar to 3D materials.

Proteins from bones, shells, and a number of microorganisms can control the nucleation and growth of inorganic structures with remarkable precision.<sup>6–8</sup> Bio-inspired assistance has also been applied to the synthesis of inorganic materials *in vitro*.<sup>7</sup> For example, Pender *et al.* reported the formation of silica- and titania-coated carbon nanotubes using a multifunctional peptide consisting of a nanotube-binding domain and an alkoxide-precipitating domain derived from the silica-precipitating protein silaffin.<sup>9</sup> These bio-inspired techniques require the identification of specific biological molecules to catalyze the formation of nanoparticles, and involve time-consuming and often complex methodologies to generate the biological template. In contrast, here we applied

the optionally available proteins from any egg as a nanoreactor for the scalable synthesis of Fe<sub>3</sub>O<sub>4</sub> nanotubes. The growth scheme of Fe<sub>3</sub>O<sub>4</sub> nanotubes is shown in Fig. 1. In the main, the surface of netlike proteins is adequate for the growth of oxide semiconductor. Proteins present an important advantage in having high affinity for metal ions, so that the particle will intercalate semiconductor precursors very efficiently.<sup>10</sup> Thus, these precursors are preconcentrated at the proteins where the chemical environment is adjusted, suitable for the subsequent semiconductor growth process. The occurrence of tubes provides an insight into the possible mechanism of their formation, suggesting that the formation of tubular structures by fundamentally similar peptides is consistent with the closure of a two-dimensional layer.<sup>11</sup>

The magnetic Fe<sub>3</sub>O<sub>4</sub> nanotubes were obtained by hydrothermal treatment of a Fe<sub>2</sub>(SO<sub>4</sub>)<sub>3</sub> solution in the presence of egg albumin. Typically, 20 ml of aqueous Fe<sub>2</sub>(SO<sub>4</sub>)<sub>3</sub> solution (0.05 M) and 5 ml of egg albumin were mixed with stirring. After stirring for 5 min, 8 ml absolute ethanol (CH<sub>3</sub>CH<sub>2</sub>OH) were added to the above solution. Finally, 10 ml of 80 wt% hydrazine hydrate solution (N<sub>2</sub>H<sub>4</sub>·H<sub>2</sub>O) were added dropwise to the above solution with vigorous stirring. After stirring for 10 min, the mixture was transferred into a 50 ml Teflon-lined stainless-steel autoclave, which was treated at 140 °C for 24 h.

The SEM images with different magnifications in Fig. 2a and b show that the as-prepared products (without purification) were mainly composed of nanotubes with a regular shape, together with a few nanosheets. The tubular structures are uniform and straight with open ends. From the open ends of the tubes, it was found that the nanotubes have thin walls. Fig. 2c shows a high-magnification SEM image of a single nanotube. The open end, as marked with the arrow, can be clearly seen. Typically, the obtained nanotubes have a uniform outer diameter of 50–60 nm and the thickness of the tube-wall

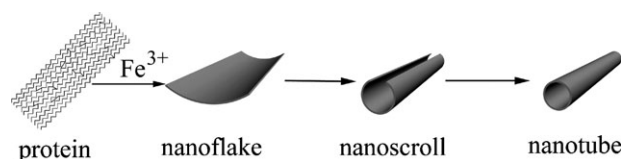


**Fig. 1** Schematic illustration of the Fe<sub>3</sub>O<sub>4</sub> nanotubes formation process using proteins as a template. Step 1: Fe<sup>3+</sup> ions and egg albumin molecules start to self-assemble and form an organic–inorganic complex. Then the Fe–N axial coordination of egg albumin N-atoms to iron ions promotes the growth of aggregates, which continue to grow into a flake structure. Step 2: the rolling up of the nanosheet gradually extends along the whole axis to form a nanoscroll. Step 3: hollow tubes are formed.

College of Chemistry and Materials Science, Anhui Key Laboratory of Functional Molecular Solids, Anhui Normal University, Wuhu, 241000, P. R. China. E-mail: bygeng@mail.ahnu.edu.cn; Fax: (+86)-553-3869303

† Electronic supplementary information (ESI) available: Experimental procedures, more SEM and TEM images of the products. See DOI: 10.1039/b813071j

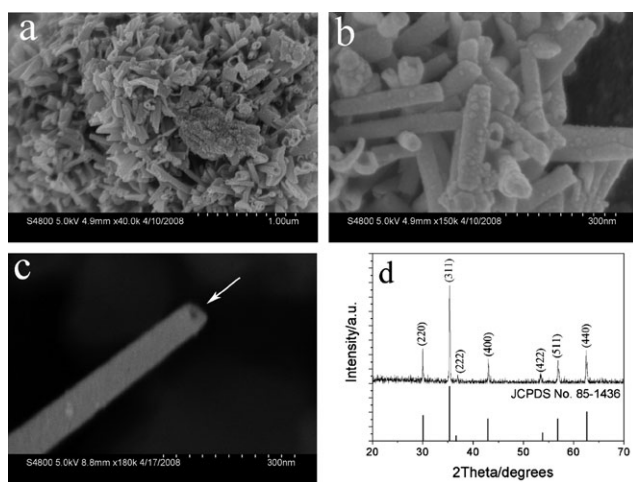


**Fig. 2** (a, b, c) SEM images of the synthesized  $\text{Fe}_3\text{O}_4$  nanotubes at different magnifications. (d) XRD pattern of the as-prepared  $\text{Fe}_3\text{O}_4$  nanotubes.

is about 15–20 nm. The XRD pattern (Fig. 2d) shows that all diffraction peaks are in good agreement with the standard Joint Committee on Powder Diffraction Standards (JCPDS) card No. 85-1436. No impurity peaks were observed, indicating that the sample was pure  $\text{Fe}_3\text{O}_4$ .

The low-magnification TEM images in Fig. 3a and b reveal that the products are pure and high-yield with tubular morphology. Two ideal nanotubes are shown in Fig. 3c, which further demonstrates that the obtained nanotubes are uniform

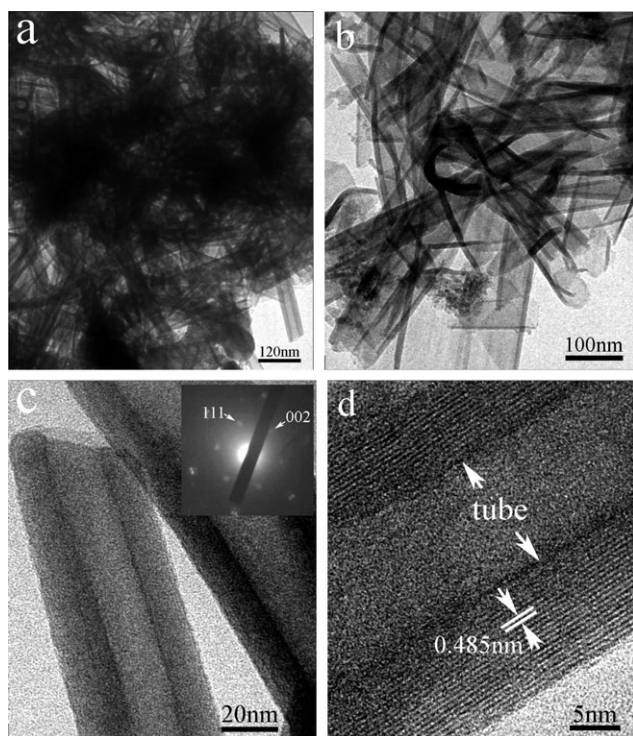


**Fig. 3** (a, b) TEM images of the synthesized  $\text{Fe}_3\text{O}_4$  nanotubes at different magnifications. (c) Magnified TEM image of two synthesized  $\text{Fe}_3\text{O}_4$  nanotubes, corresponding SAED pattern in inset. (d) HRTEM image of a single  $\text{Fe}_3\text{O}_4$  nanotube.

along their entire length and with tube-wall thickness about 15–20 nm. The SAED pattern (the inset of Fig. 3c) obtained along a typical individual nanotube confirms the  $\text{Fe}_3\text{O}_4$  to be single crystalline.

The HRTEM image of a single  $\text{Fe}_3\text{O}_4$  nanotube further supports the single-crystalline nature of these nanotubes (Fig. 3d). The lattice fringes ( $\sim 0.485$  nm) observed in this image agree well with the separation between the (111) lattice planes. Combined with the SAED results this confirmed that the nanotubes grow along [110], one of the easy magnetic axes of  $\text{Fe}_3\text{O}_4$ .

In order to prove that egg albumin played a critical role in the synthesis of  $\text{Fe}_3\text{O}_4$  nanotubes, we performed a series of experiments to explore the formation process (see the Supporting Information, Fig. S1†). It was found that uniform nanoparticles were obtained without using the egg albumin. On increasing the amount of egg albumin, the morphology of the products evolved from nanoflakes to nanotubes. The time-dependent morphology evolution of the products is shown in Supporting Information, Fig. S2.† The results showed that the morphologies of the products changed from nanoflakes to nanoscrolls and then to nanotubes. The above proof indicates that tubular  $\text{Fe}_3\text{O}_4$  nanostructures are formed from the two-dimensional flake-like precursors based on a “rolling-up” mechanism.

It has been shown that in nature, protein interactions not only direct nucleation of inorganic materials, but also control the crystal type, face, and size, even of metastable forms, all in aqueous solutions and under ambient conditions.<sup>12,13</sup> On the basis of the above experimental results, we propose a tentative mechanism for the formation of  $\text{Fe}_3\text{O}_4$  nanotubes comprising the following steps. Initially,  $\text{Fe}^{3+}$  ions and egg albumin molecules start to self-assemble and form an organic–inorganic complex in the aqueous solution of ethanol. With the diffusion of hydrazine hydrate into water, ethanol molecules form dimers, and the dimers aggregate with egg albumin molecules. The Fe–N axial coordination of egg albumin N-atoms to iron ions promotes the growth of aggregates, which continue to grow into a flake structure mainly driven by crystal packing force and stacking interactions among adjacent iron atoms. With the increase of temperature, hydrogen bonds and peptide bonds start rupturing, and this induces different stacking interactions among adjacent iron atoms. The difference between the strong stacking interactions in the three dimensions leads to the different growth rates that eventually result in the formation of tubes.

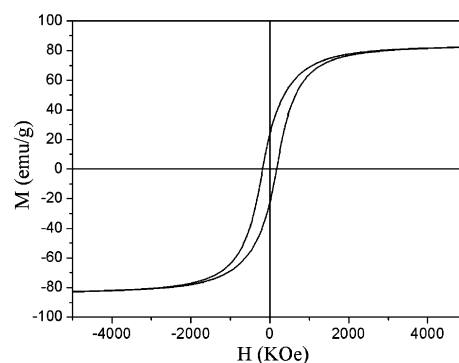


**Fig. 4** Magnetic hysteresis curves measured at room temperature for  $\text{Fe}_3\text{O}_4$  nanotubes.

Fig. 4 shows magnetic hysteresis curves for the as-synthesized nanotubes measured at room temperature. It can be clearly seen that the products have a saturation magnetization of  $81.7 \text{ emu g}^{-1}$ , which is lower than that of bulk  $\text{Fe}_3\text{O}_4$  ( $85\text{--}100 \text{ emu g}^{-1}$ ).<sup>1</sup> The deviation is likely due to the nanostructured  $\text{Fe}_3\text{O}_4$ , for the magnetization reduces with the decrease of the particle sizes.

The coercivity value amounts to 168.1 Oe for  $\text{Fe}_3\text{O}_4$  nanotubes. It is reported that 1D nanostructures have increased anisotropies in both the shape anisotropy and the magneto-crystalline, which exert influence on their magnetic properties. Shape anisotropy can increase the coercivity. Enhanced anisotropy induces large magnetic coercivity, where the magnetic spins are preferentially aligned to the long axis and their reversal to the opposite direction requires higher energies than those for spheres.<sup>14</sup> Here, as compared to the coercivity value of the bulk  $\text{Fe}_3\text{O}_4$  (115–150 Oe),<sup>15</sup> the  $\text{Fe}_3\text{O}_4$  nanotubes exhibit higher values, which may be attributed to their tubular structures. From the results discussed above, it is clear that the as-prepared nanotubes have high magnetic properties, making it possible for them to be used in biotechnology and biomedicine.

In summary, magnetic  $\text{Fe}_3\text{O}_4$  nanotubes have been synthesized by an albumen-assisted growth process. This approach provides a simple, novel, and feasible method for the preparation of stable, magnetic nanotubes. This approach not only enriches magnetite chemistry, but also provides a new strategy to synthesize single-crystalline nanotubes of nonlamellar-structured materials, which could be applicable to the synthesis of other inorganic tubular nanostructures.

This work was supported by the National Natural Science Foundation of China (20671003), the Foundation of Key Project of Natural Science of Anhui Education Committee

(2006kj041a), the Education Department of Anhui Province (2006KJ006TD) and the Program for Innovative Research Team in Anhui Normal University.

## Notes and references

- 1 S. Iijima, *Nature*, 1991, **354**, 56.
- 2 (a) C. H. Ye, G. W. Meng, Z. Jiang, Y. Wang, G. Z. Wang and L. D. Zhang, *J. Am. Chem. Soc.*, 2002, **124**, 15180; (b) C. H. Ye, Y. Bando, G. Z. Shen and D. Golberg, *Angew. Chem., Int. Ed.*, 2006, **45**, 4922; (c) N. G. Chopra, R. J. Luyken, K. Cherrey, V. H. Crespi, M. L. Cohen, S. G. Louie and A. Zettl, *Science*, 1995, **269**, 966; (d) R. Tenne, L. Margulis, M. Genut and G. Hodes, *Nature*, 1992, **360**, 444; (e) S. Zhang, L. M. Peng, Q. Chen and G. Dawson, *Phys. Rev. Lett.*, 2003, **91**, 256103.
- 3 (a) J. Q. Hu, Y. Bando, Z. W. Liu, D. Golberg and T. Sekiguchi, *Angew. Chem., Int. Ed.*, 2004, **43**, 63; (b) J. Goldberger, S. W. Lee and P. D. Yang, *Nature*, 2003, **424**, 599.
- 4 Z. Q. Liu, S. Han, C. Li, B. Lei and C. W. Zhou, *J. Am. Chem. Soc.*, 2005, **127**, 6.
- 5 B. Mayers and Y. N. Xia, *Adv. Mater.*, 2002, **14**, 279.
- 6 V. Bansal, P. Poddar, A. Ahmad and M. Sastry, *J. Am. Chem. Soc.*, 2006, **128**, 11958.
- 7 S. P. Chandran, M. Chaudhary and M. Sastry, *Biotechnol. Prog.*, 2006, **22**, 577.
- 8 C. B. Mao, J. D. Solis, B. Iverson and A. M. Belcher, *Science*, 2004, **303**, 213.
- 9 M. J. Pender, L. A. Sowards, M. O. Stone and R. R. Naik, *Nano Lett.*, 2006, **6**, 40.
- 10 H. C. Tsai and R. A. Doong, *Biosens. Bioelectron.*, 2005, **20**, 1796.
- 11 S. Scanlon and A. Aggeli, *Nano Today*, 2008, **3**, 22.
- 12 G. Falini, S. Albeck, S. Weiner and L. Addadi, *Science*, 1996, **271**, 67.
- 13 J. Aizenberg, A. J. Black and G. M. Whitesides, *Nature*, 1999, **398**, 495.
- 14 S. J. Park, S. Kim, K. Char and J. Hyeon, *J. Am. Chem. Soc.*, 2000, **122**, 8581.
- 15 B. Y. Geng, J. Z. Ma and L. D. Zhang, *Appl. Phys. Lett.*, 2007, **90**, 043120.